Plasma Medicine, 5(2–4): 125–143 (2015)

Slow Molecular Transport of Plasma-Generated Reactive Oxygen and Nitrogen Species and O_2 through Agarose as a Surrogate for Tissue

Jun-Seok Oh,[1,2,†] Endre J. Szili,[3,4,†] Satsuki Ito,[1] Sung-Ha Hong,[3,4] Nishtha Gaur,[3,4] Hiroshi Furuta,[1,2] Robert D. Short,[3,4,*] & Akimitsu Hatta[1,2,*]

[1]Department of Electronic and Photonic Systems Engineering, Kochi University of Technology, 185 Miyanokuchi, Tosayamada-cho, Kami-shi, Kochi 782-8502, Japan; [2]Center for Nanotechnology, Research Institute of Kochi University of Technology, 185 Miyanokuchi, Tosayamada-cho, Kami-shi, Kochi 782-8502, Japan; [3]Future Industries Institute, University of South Australia, Adelaide, South Australia 5095, Australia; [4]Wound Management Innovation Cooperative Research Centre, Australia

[†]Jun-Seok Oh and Endre J. Szili are co–first authors.

*Address correspondence to: Robert D. Short, University of South Australia, Future Industries Institute, Mawson Lakes Campus, Mawson Lakes SA 5095; Tel.: +61 8 8302 3190; rob.short@unisa.edu.au; Akimitsu Hatta, Department of Electronic and Photonic Systems Engineering, Kochi University of Technology, 185 Miyanokuchi, Tosayamada, Kami, Kochi 782-8502, Japan; Tel.: +81 887 57 2113; hatta.akimitsu@kochi-tech.ac.jp

ABSTRACT: The helium (He) atmospheric-pressure plasma jet (APPJ) delivery of reactive oxygen and nitrogen species (RONS) and molecular oxygen (O_2) in deionized (DI) water was monitored in real time using in situ UV absorption spectroscopy. The He APPJ was used to treat DI water directly and through an agarose target as a surrogate for tissue (e.g., a skin barrier). For direct treatment, the RONS were generated immediately in the DI water, and the concentration of RONS continued to increase during the He APPJ treatment. But there was only a very minor increase in the total RONS concentration detected after the plasma and gas flow were switched off. The agarose target delayed the generation of RONS into the DI water, but the total RONS concentration continued to increase long after (25 min) the plasma and gas flow were switched off. Direct treatment deoxygenated the DI water, whereas treatment through agarose resulted in oxygenation of the DI water. A dynamic change in the ratio of H_2O_2, NO_2^-, NO_3^-, and O_2 was detected in the DI water during He APPJ treatment and 25 min after the He and gas flow were switched off for both direct and through-agarose treatment. These results have implications for the plasma treatment of real tissue where the dynamic changes in the RONS and O_2 concentrations within the tissue and tissue fluid could affect cellular and physiological processes.

KEY WORDS: RONS transport, oxygenation, deoxygenation, agarose target, in situ UV absorption spectroscopy

I. INTRODUCTION

The potential of atmospheric-pressure plasma (APP)[1,2] to aid in the treatment of problematic indications, including nonhealing chronic wounds, bacterial infections, dental decay, and cancer, is being explored.[3,4] This potentially opens the door to a new multidisciplinary field of research referred to as *plasma medicine*.[5–13]

1947-5764/15/$35.00

The efficacious effects of plasma are strongly linked to the reactive oxygen species (ROS) and reactive nitrogen species (RNS), or collectively, RONS, that are generated by APP in the gas phase, in the tissue fluid, and within tissue.[7] RONS are generated within our own cells and are known to regulate key biochemical pathways that are vital to the maintenance of normal physiological function and the fight against disease.[14] Graves has summarized the biochemistry of how plasma-generated RONS might activate or deactivate a number of well-established biological processes.[15] Because APP can be operated with the neutral gas temperature at or close to ambient,[16–18] the RONS that are generated by APP can be delivered to different biomedically relevant targets, including living tissue, soft biofilms, and tissue fluid, without causing any thermal damage.

Arguably the most common plasma source used in plasma medicine is the APP jet (APPJ), where a plasma plume is launched into the air for treatment.[19–26] APPJs have been widely investigated as a new therapeutic technology in the treatment of cancer[27–33] and wound healing.[34,35] Although the diameter of the APPJ is generally less than 1 mm, the APPJ usually treats a much larger area, with a diameter measured in centimeters, because of gas turbulence at the gas-target interface.[36–38] APPJs are usually operated with an inert argon (Ar) or helium (He) gas. The long extension of the plasma plume and the gas flow enables RONS to be delivered by the APPJ over a relatively long distance (several centimeters) from the target surface.[23] The delivery of RONS is generally confined to a small area of approximately 10 mm across the target surface.[11] But this changes according to the gas flow that influences the spread of RONS across the target surface because of gas turbulence as mentioned earlier.[36,37]

To date most of the research has focused on understanding the role of plasma-generated RONS in plasma medicine at the molecular and cellular level.[39–42] Arguably, less attention has been paid to understanding the interactions of plasma at the tissue level. Although plasma-generated RONS have been shown to intervene in cellular processes, it is not known how the plasma-generated RONS can be delivered deep into tissue for disease treatment. Because many of the plasma-generated RONS have short lifetimes and diffusion lengths and will react quickly upon contact with the target surface, it is difficult to understand how, for example, an APPJ can destroy microorganisms within biofilms[43–48] and cancerous cells within sizable tumors.[13,14] Therefore, in an attempt to better understand the mechanisms underlying the use of plasma in medical applications at the tissue level, we have developed a straightforward and low cost method to analyze the delivery of RONS into tissue. We have employed a simple experimental setup where a He APPJ is used to treat an agarose target that is placed on top of a cuvette filled with deionized (DI) water. The transport of RONS through the agarose target into the DI water is measured in real time by UV absorption spectroscopy analysis of the DI water.[3,4,51] Agarose is commonly used to mimic different tissues and tumors.[52–58] For example, a team at Drexel University has previously used agarose targets to investigate plasma-tissue interactions.[59,60] We have previously demonstrated that the He APPJ can deliver RONS to significant (>3 mm) depths within agarose. This suggests that plasma-generated RONS may directly interact with cells embedded within tissue, rather than

indirectly through a cascade of biomolecular reactions and signaling events triggered by surface stimulation and propagated into the tissue.[4]

Understanding the delivery of RONS into tissue is also important from a patient's perspective, where for safety reasons, defined doses of plasma or even its constituent species will eventually be mandated. To the best of our knowledge, dynamic changes in the RONS concentration and composition and O_2 concentration within plasma irradiated tissues has not been systematically studied. Yet, these need to be understood, as they have the potential to significantly affect the medical outcome.

In our previous research we quantified the total RONS delivered into the DI water. However, the He APPJ generates a mixed population of RONS with different levels of reactivity. Therefore, in the treatment of living tissue, we expect that cells embedded within the tissue will respond to the plasma treatment, not only according to the total RONS concentration but also to the ratio of the different RONS generated in the tissue or tissue fluid. For example, Reuter has shown that HaCaT cell viability is more sensitive to plasma-generated ROS than RNS.[61]

In this paper, we used time-resolved UV absorption spectroscopy to quantify the specific RONS that are generated directly in DI water or transported through an agarose target into DI water during the He APPJ treatment (Scheme 1). The purpose of the agarose target is not to mimic a specific tissue type, but to act as a barrier (similar to a skin barrier) between the APPJ and the DI water to inhibit the passage of the RONS into the DI water. The RONS investigated in this paper were H_2O_2, NO_2^-, NO_3^-, which are the major (longer-lived) RONS generated by APP in DI water.[62–66] In addition to RONS, Collet et al. has shown that a He APPJ induces tissue oxygenation in live mice.[67] The results in our previous paper, involving the He APPJ treatment of DI water through an agarose target, support the finding by Collet et al. that a He APPJ is effective in oxygenating the tissue.[3] However, the molecular oxygen (O_2) concentration was not quantified in our previous study. Therefore, we also investigated the change in the O_2 concentration in the DI water during direct and through-agarose He APPJ treatment of DI water. Our results are discussed in the context of how the plasma delivery of RONS and O_2 into tissue and tissue fluid may influence the effects of plasma in the treatment of diseased tissue.

II. EXPERIMENTAL METHODS

A. He APPJ

The He APPJ consisted of a glass tube with a length of 15 cm, in which the inner diameter was tapered from 4 mm to 800 μm (Scheme 1). The glass tube has a metallic external ring electrode with a length of 15 mm, wound onto the glass tube, 4 cm from the end of capillary. He gas was fed into the glass tube with a fixed flow rate of 1 SLM. A capillary dielectric barrier discharge was generated using a high-voltage bipolar square wave pulse of 7 kV (peak-to-peak) applied to the external electrode with a fixed frequency of 10 kHz. The driving voltage and discharge current were measured with a high-voltage

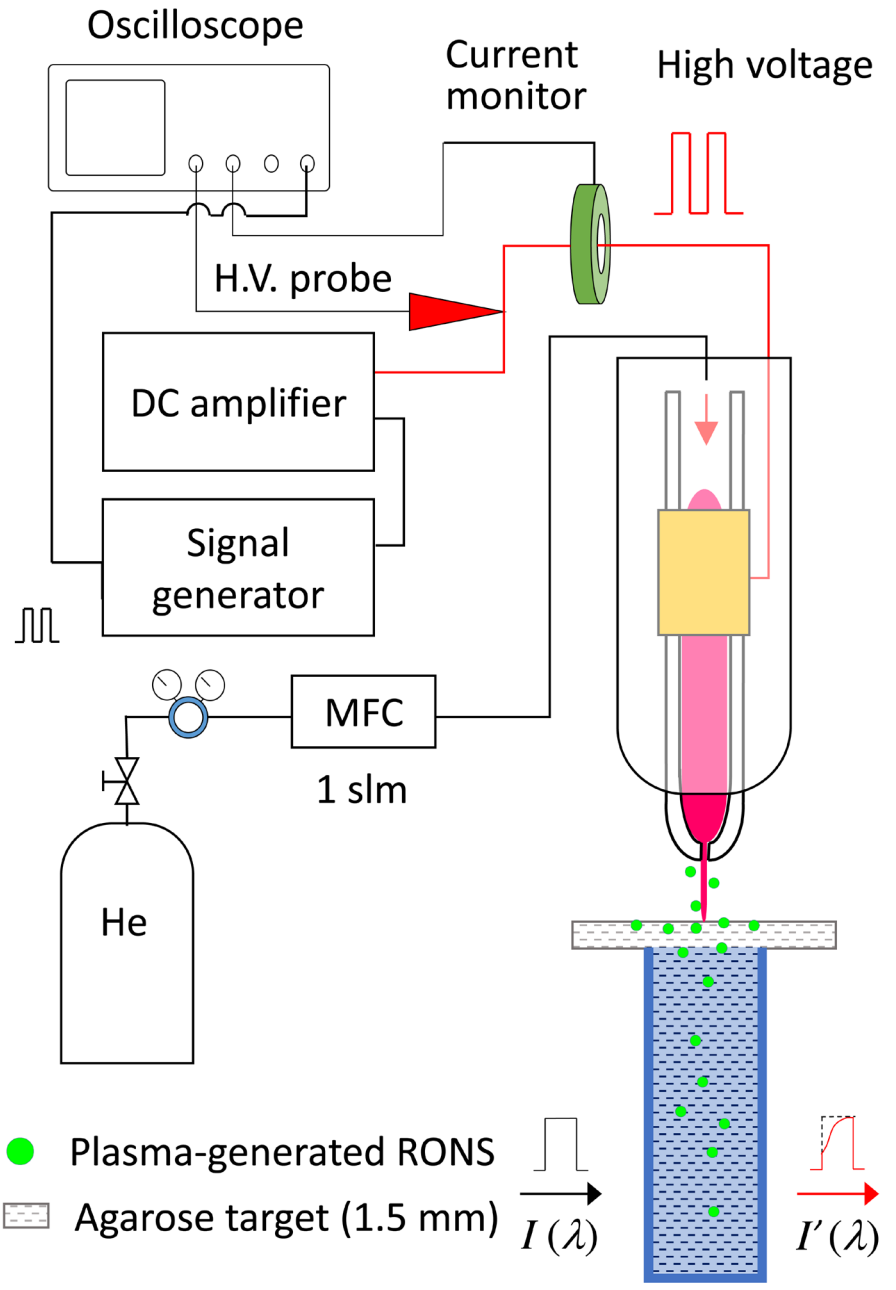

SCHEME 1: Experimental setup employed in the in situ UV absorption spectroscopy method for monitoring the transport of RONS through a 1.5 mm thick agarose target into DI water during He APPJ treatment. The agarose target on top of the cuvette was removed for the direct treatment of the DI water.

probe (Tektronix P6015A) and a conventional current monitor (Pearson 2877), respectively. More details on the current and voltage measurements can be found in previous publications.[18,24,25] Both positive and negative discharge currents were observed during a voltage cycle. For all experiments, the He APPJ treatment was 5 or 12 min, after which both the plasma and He gas flow were switched off. When the plasma and He gas flow were switched off at 5 min, all of the RONS were still contained within the agarose target; whereas at 12 min, some of the RONS were already transported through the agarose target into the DI water underneath it.[3,4]

B. Agarose Target

A 2% (w/v) agarose target was prepared by dissolving 20 mg/mL agarose powder (Sigma-Aldrich, catalogue number A9539) in DI water (18.2 MΩ-cm) purified through a Millipore Direct-Q system (model number ZRQ50PO30). The solution was heated (typically for 1–2 min) in a conventional microwave oven until all the powder was dissolved. The solution was cooled before pouring 15 mL of solution into an 85 mm diameter (plastic) petri dish. The plate was gently agitated to enable the solution to evenly spread over the bottom of the dish, while taking precaution not to create air bubbles in the solution. The agarose was allowed to set at 4ºC for 12 hours before use. Square sections of approximately 3 × 3 cm^2 were cut using a scalpel and removed with a polytetrafluoroethylene tweezer, taking care not to tear the agarose. The agarose targets were stored in DI water at 4°C until use. The thickness of the agarose target was 1.5 mm, as measured with a vernier caliper.

C. *In Situ* UV Absorption Spectroscopy

The quantitative measurement of RONS in the DI water was obtained by UV absorption spectroscopy. A conventional double-beam UV-Vis spectrometer (U-3900, Hitachi) was used to detect the transmittance of the DI water up to 30 min in real time. The spectral resolution was 0.2 nm and the scan speed was 120 nm min^{-1}. The spectrometer can detect a broad wavelength range from 190–900 nm, but no significant absorption was detected above 300 nm. Therefore, the analysis of the DI water was performed from 190 nm up to 400 nm. The measurements were performed in quartz cuvettes (100-QS, Hellma Analytics) filled with 4 mL of DI water. The lowest transmittance of the quartz cuvettes was 82% at the shortest wavelength of 190 nm, and transmittance for the whole wavelength range was 85%. Absorbance, A, was defined by $A = -\log(I/I_0)$, where I is transmittance of the DI water exposed to the APPJ and I_0 is transmittance of the DI water before the APPJ treatment. For through-agarose APPJ treatment, the agarose target was placed on the top of the quartz cuvette filled with the DI water so that the agarose target and DI water remained in contact during the measurements. The maximum measurement period was 30 min, which included the 5 or 12 min He APPJ treatment (i.e., 5 or 12 min He APPJ treatment + 25 or 18 min with plasma and gas flow off).

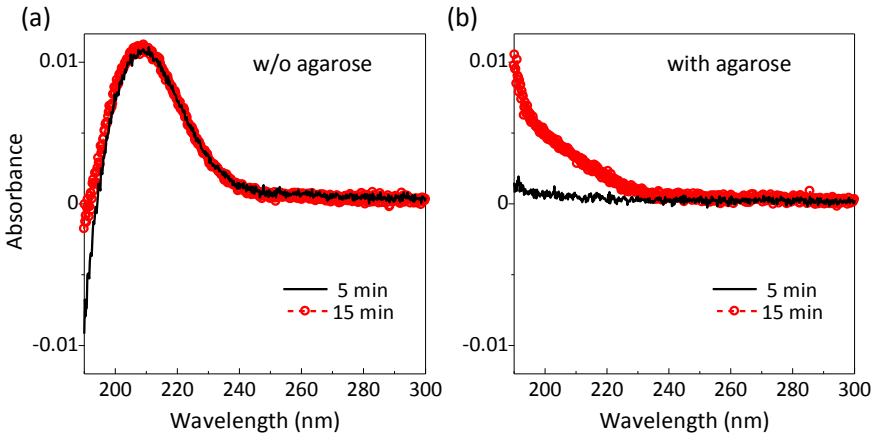

FIG. 1: UV absorption profile of DI water treated with (a) the He APPJ directly in contact with the DI water (w/o agarose), and (b) in contact with the 1.5 mm thick agarose target (with agarose). Plasma was applied directly for 5 min in (a) and (b). Both the plasma and gas flow were switched off after 5 min. The increase in the absorption profile indicates an increase in the RONS concentration in the DI water. Measurements were taken at 5 and 15 min (i.e., 10 min after the plasma and gas flow were switched off).

III. RESULTS AND DISCUSSION

A. UV Absorption Profile

Figure 1(a) is a typical UV absorption spectrum from 190 to 300 nm for DI water directly treated with the He APPJ for 5 min with measurements taken at time points of 5 min and 15 min (i.e., 10 min post He APPJ treatment). After 5 min of He APPJ treatment, a broad prominent peak was detected at 210 nm. But at the lower wavelength range of 190–195 nm, the absorbance was negative. At 15 min, the absorbance in the range of 190–195 nm had increased, and the absorbance between 195 and 300 nm did not change. We will discuss the cause of the negative absorbance in sections 3.C and 3.D. Figure 1(b) shows the corresponding UV spectra for DI water after through-agarose He APPJ treatment. From this figure, we can see that at 5 min, the total absorbance was much lower than that seen in DI water directly treated with the He APPJ. At 15 min, there was a marked increase in the UV absorbance, but the profile of the UV spectrum was different to the profile of the DI water directly treated with the APPJ. These results indicate that the He APPJ generated RONS directly in the DI water through a relatively fast process and only during the plasma-on period. Whereas for through-agarose treatment, the RONS were transported into the DI water through a slower process and continued to be transported into the DI water underneath the agarose target 10 min after the plasma and gas flow were switched off. In addition to the difference in the RONS transport rate, the UV absorption profiles in Figure 1(a) and 1(b) were markedly different for direct versus through-agarose treat-

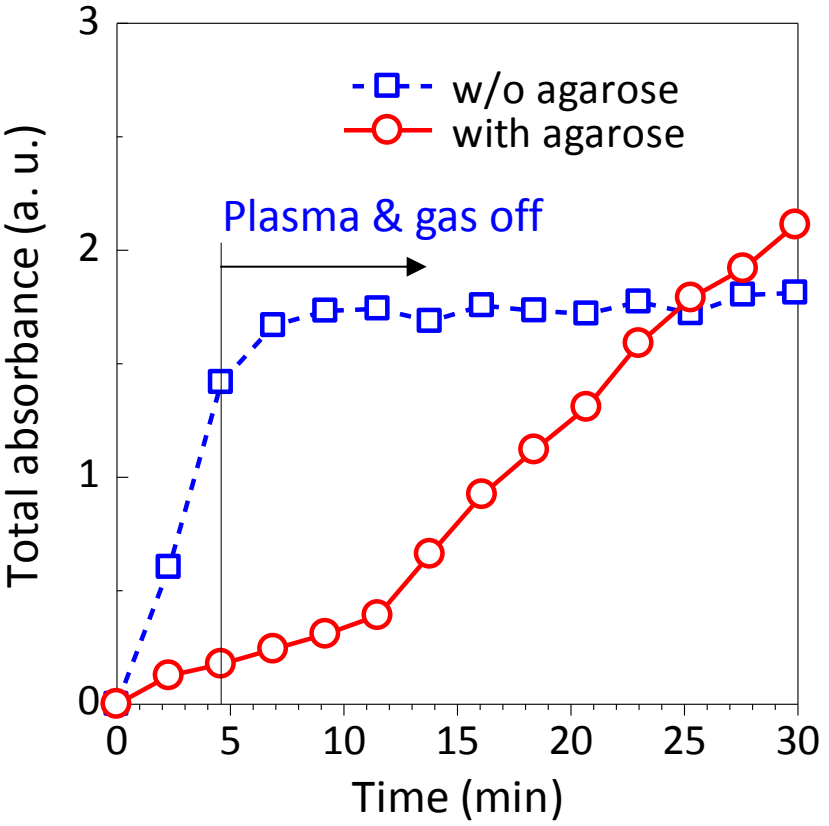

FIG. 2: Time-dependent change in the total UV absorbance between 190 and 400 nm during direct (without agarose) and through-agarose treatment (with agarose) of the DI water. The plasma and He gas flow were switched off after 5 min.

ment. These results indicate that different RONS or the concentration of RONS, or both, were delivered by the He APPJ directly into the DI water, in comparison to the RONS delivered through the agarose target into the DI water.

B. Time-Dependent Transport of RONS

To further investigate the generation and transport of RONS into the DI water, the total absorbance (T_{abs}) of the UV spectrum from 190 to 400 nm was plotted up to 30 min (5 min He APPJ treatment + 25 min post treatment). Figure 2 shows the time-dependent change of the T_{abs}, with and without the agarose target. For the direct He APPJ treatment of the DI water, the T_{abs} increased linearly up to 5 min, which corresponded to the plasma on time of 5 min. The T_{abs} showed very minor increase, but remained constant, after the plasma and He gas flow were switched off. In comparison, for through-agarose treatment, there was a lag period of 12 min where the T_{abs} did not significantly increase. After

the 12-min lag period, the T_{abs} increased linearly for the remainder of the measurement time. The time lag was induced by an accumulation of RONS within the agarose target before a subsequent (time-lagged) release into DI water.[4] The T_{abs} increased at a slower rate for through-agarose treatment between 12 and 30 min compared to direct treatment of the DI water between 0 and 5 min. But the final T_{abs} value, measured at 30 min, was higher for through-agarose treatment compared to the direct treatment of the DI water. These results indicate that the direct He APPJ treatment generated RONS in the DI water by a fast process that could be through fast solvation of the RONS from the gas phase into the DI water[19] or UV photolysis, or both.[20] But we suspect that fast solvation is the major process. In our previous work, RONS were not generated in the DI water after He APPJ treatment of the DI water through a quartz plate (with 90% transmittance from 190 to 900 nm, ShinEtsu VIOSIL) that blocked the gas flow, thus preventing solvation of RONS that were generated in the gas phase.[4]

In comparison, we argue that RONS were transported through the agarose target by a slow molecular transport process. Since the final T_{abs} was higher for through-agarose treatment, either new RONS were generated within the agarose target that were not generated directly within the DI water or other molecular species were transported through the agarose that contributed to the UV absorption spectrum. This is discussed further in section 3.D.

C. UV Absorption Spectra of RONS and O_2

Figure 3 shows the UV spectra of 1 mg/L H_2O_2, $NaNO_2$, and HNO_3, which are the major longer lived RONS that are generated by APP in DI water, as well as O_2.[63–67] (We repeated the measurement of the absorption spectra of the reference solutions multiple times to ensure the reliability of the absorption spectra for the curve fitting.)[68] These measurements were used to inform the subsequent peak fitting of the H_2O_2, NO_3^-, NO_2^- and O_2 components in the UV spectra of the DI water treated directly with the He APPJ or through agarose. Over the concentration range relevant to this study, there was a linear increase in the UV absorbance spectra as the concentrations of these RONS and O_2 were increased in the DI water (data not shown). The optimum fit for the O_2 UV absorption spectrum was determined with two approaches. In the first approach, 0.5 SLM of O_2 was purged into 4 mL of DI water for 30 min. The O_2 treatment resulted in an increase in the intensity of the UV absorption spectrum between 190 and 210 nm. In the second approach, the DI water was treated with 1 SLM of the neutral He gas flow alone (i.e., with plasma off), which resulted in a decrease in the intensity of the UV absorption spectrum from 190 to 210 nm (data not shown). This result indicates the He gas flow deoxygenates the DI water. After 15 min, the UV absorption stopped decreasing, which indicates that all of the dissolved O_2 (~8 mg/L at atmospheric pressure and room temperature) was removed from the DI water, or that it was not possible to further deoxygenate the water. Since direct He APPJ treatment of the DI water resulted in a similar negative UV absorbance between 190 and 195 nm in Figure 1(a), this result indicates that the He APPJ deoxygenated the DI water, and we presume this is due to the He gas

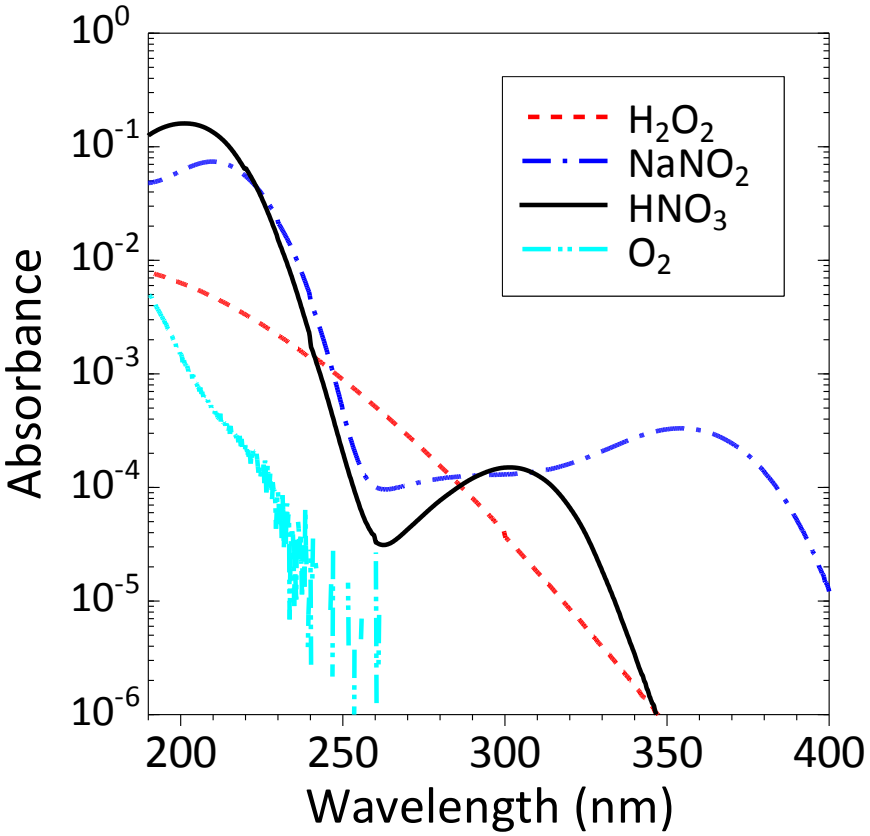

FIG. 3: UV absorption spectra of 1 mg/L of H_2O_2, NO_3^-, NO_2^-, and O_2 in DI water.

flow. But when the He gas flow was blocked by the agarose target, the UV absorbance immediately increased in the range 190–195 nm in Figure 1(b), indicating that the He APPJ oxygenated the DI water.

D. Concentrations of RONS and O_2

Based on Figure 3, the UV absorption spectrum of DI water treated directly with the He APPJ or through-agarose was fitted to a curve with a program developed in-house to obtain the individual curves for H_2O_2, NO_3^-, NO_2^-, and O_2.[22] Figure 4 shows the result of the curve fitting for DI water directly treated with the He APPJ. Curve fitting was performed at 7 min and 25 min, as shown in Figures 4(a) and (b), respectively, where the plasma and gas flow were switched off at 5 min. At 7 min, the order of the RONS concentration from highest to lowest was H_2O_2 (0.62 mg/L, NO_2^- (0.074 mg/L), and NO_3^- (0.029 mg/L). These concentrations did not significantly change at the 25 min time point. At 7 min, the O_2 concentration was 4.13 mg/L, which was approximately half the

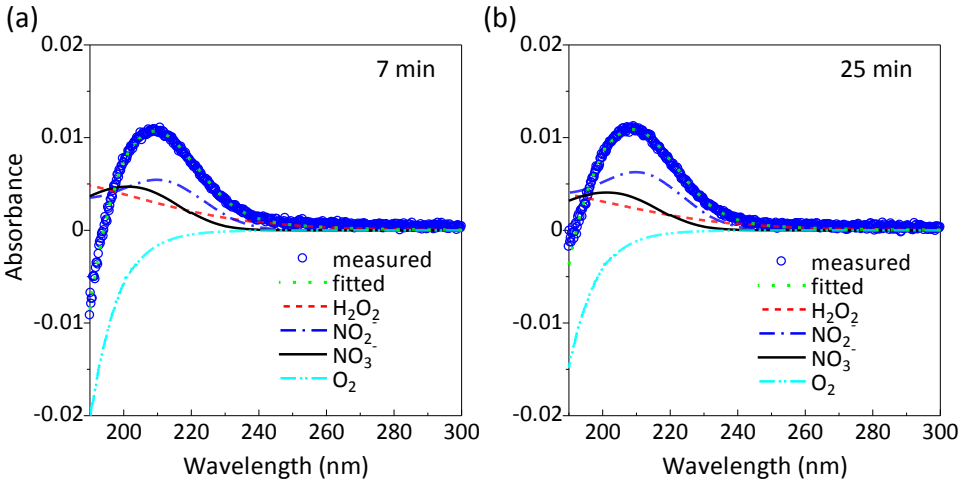

FIG. 4: Curve fitting of the UV absorption spectra of the DI water treated directly with the He APPJ for 5 min. The fitted curve is shown for (a) the 7 min (5 min He APPJ + 2 min plasma and He gas flow off) and (b) 25 min (5 min He APPJ + 20 min plasma and He gas flow off) measurement time points.

concentration for DI water (~8 mg/L). At 25 min the O_2 concentration was 5.22 mg/L, which was still below the original O_2 concentration in the DI water.

Figure 5 shows the curve-fitting data for through-agarose treatment. At 7 min in Figure 5(a), the intensity of the UV absorbance spectrum was low, indicating that very little or no RONS were transported into the DI water at this time point. This result was expected from the time-resolved T_{abs} data in Figure 2 that showed only a very small quantity of RONS were transported through the agarose into the DI water within the first 12 min. A close inspection of Figure 5(a) revealed that the UV absorbance increased between 190 and 210 nm, corresponding to H_2O_2 and O_2 concentrations of 0.16 mg/L and 8.01 mg/L, respectively. At 25 min, there was a significant increase in the concentration of RONS in the DI water. The RONS concentration at 25 min from highest to lowest was H_2O_2 (0.67 mg/L), NO_3^- (0.016 mg / L), and NO_2^- (0.005 mg/L); whereas the O_2 concentration of the DI water was 8.17 mg/L.

For both direct and through-agarose treatments, H_2O_2 was detected at the highest level, which was expected from our own studies and those by other groups.[69–71] Currently, we do not know why the NO_2^-:NO_3^- ratio was higher for direct treatment than through-agarose treatment. We speculate that the RNS undergo reactions that favor the generation of NO_3^- during their slow molecular transport through the agarose target or the generation of NO_3^- is more favorable in an O_2 rich environment; or possibly both processes support the differences in the ratios.

The oxygenation of the DI water below the agarose target cannot be attributed to neutral O_2 molecules. In a control experiment, the agarose target was treated with 0.5 SLM of O_2 gas flow alone. But this did not change the UV absorbance, even after a 30-

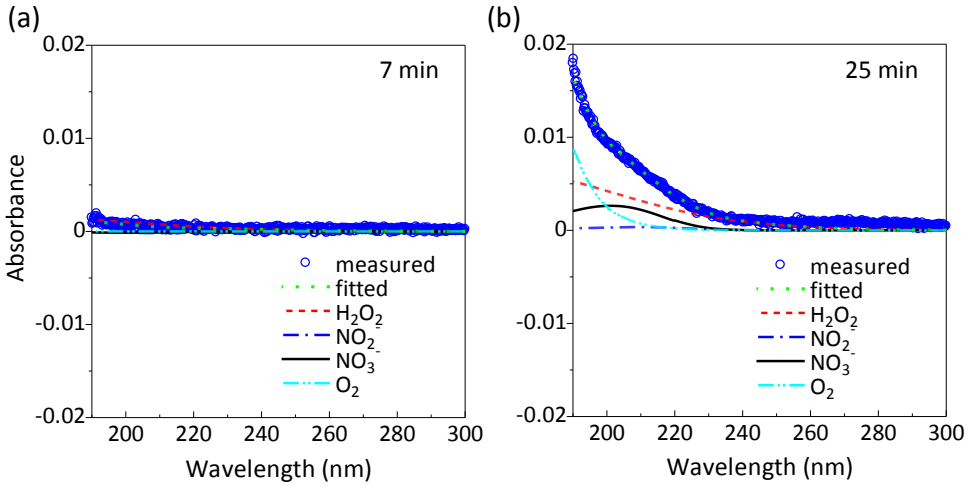

FIG. 5: Curve fitting of the UV absorption spectra of the DI water treated with the He APPJ through an agarose target for 5 min. The fitted curve is shown for (a) the 7 min (5 min He APPJ + 2 min plasma and He gas flow off) and (b) 25 min (5 min He APPJ + 20 min plasma and He gas flow off) measurement time points.

min treatment with O_2 gas flow. Therefore, for through-agarose treatment, it could be that the positively or negatively charged oxygen species (O^+, O_2^+, O^-, O_2^-) increased the dissolved O_2 concentration in the DI water (upon recombination).

E. Time-Dependent Generation of RONS

The curve-fitting program was used to automatically fit the UV spectra. This enabled us to plot the different RONS that were generated by the He APPJ over a wide time range of 0–30 min for both direct and through-agarose plasma treatment. The He APPJ treatment was 5 min (Figure 6) or 12 min (Figure 7), after which, the plasma and He gas flow were switched off.

In Figure 6, it can be seen that the H_2O_2, NO_2^- and NO_3^- concentrations all increased linearly in the DI water during direct He APPJ treatment (without agarose). During the time that plasma and He gas flow were off from 5 to 30 min, the H_2O_2 concentration stopped increasing and remained stable; the NO_2^- concentration continued to increase at the same rate for an additional 2 min before increasing at a much reduced rate; and the NO_3^- concentration decreased at a relatively slow rate. The original O_2 concentration continually decreased during the He APPJ treatment (first 5 min), but increased at a relatively slow rate after the plasma and He gas flow were switched off. Similar trends were observed for DI water treated directly with the He APPJ for 12 min, as shown in Figure 7.

For through-agarose treatment, a lag period of approximately 12 min was evident,

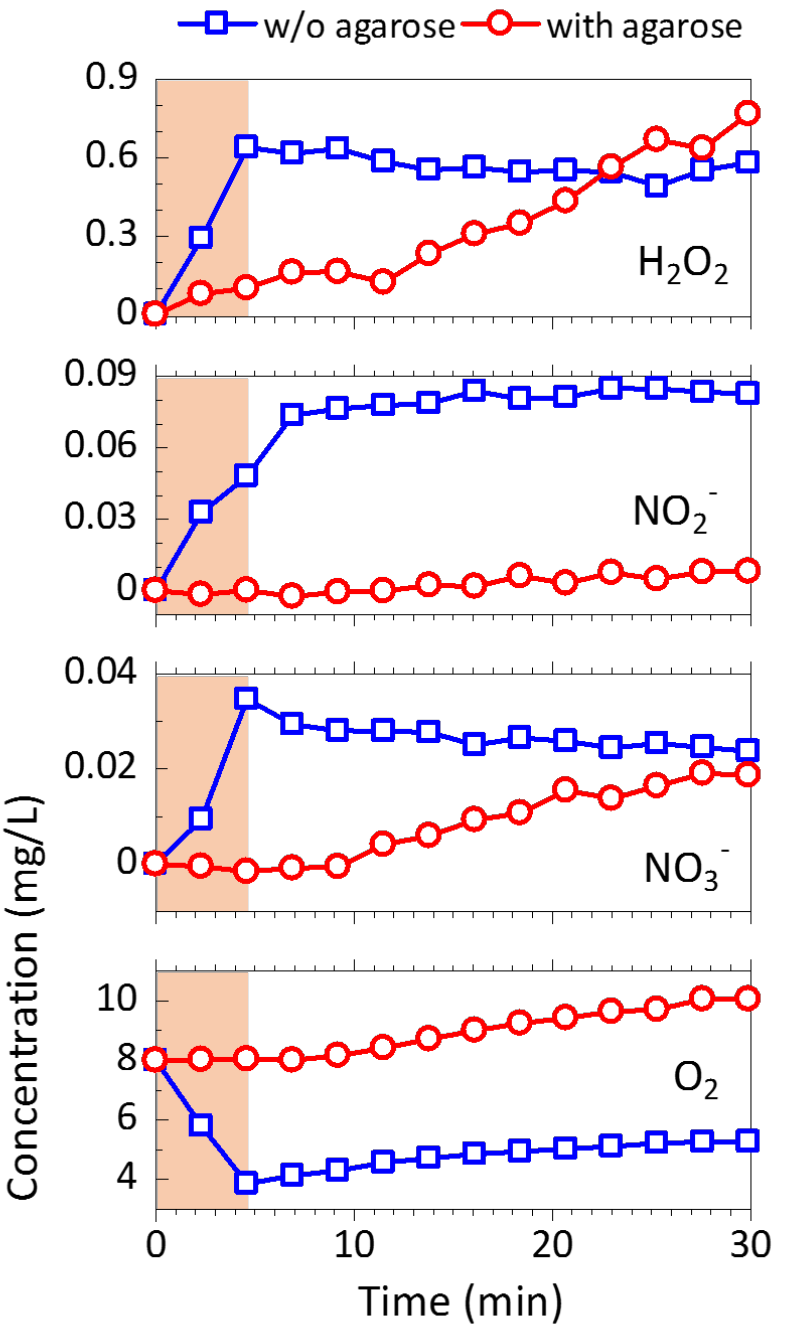

FIG. 6: Time-dependent change in the concentration of H_2O_2, NO_2^-, NO_3^-, and O_2 in DI water treated directly with the He APPJ (without agarose) or through an agarose target (with agarose). The He APPJ treatment time was 5 min as highlighted in the graphs.

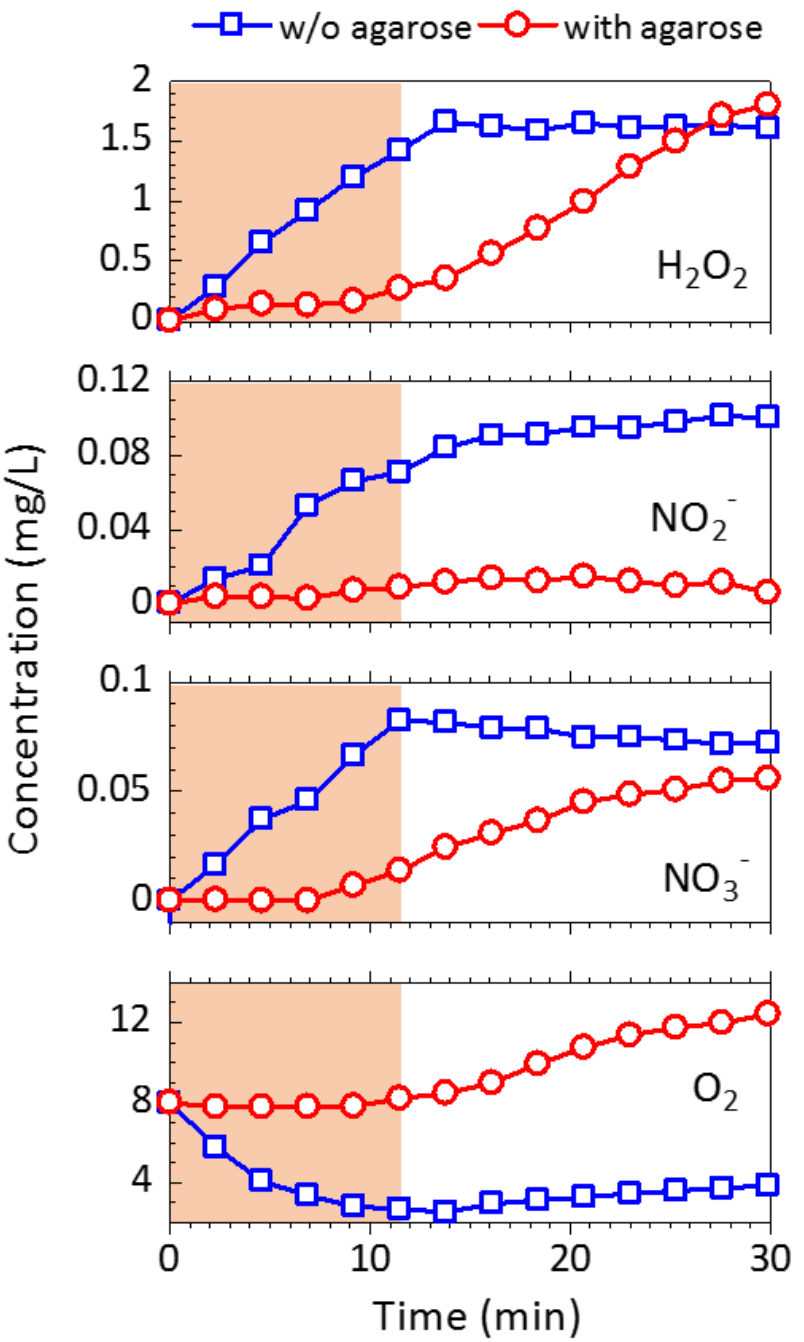

FIG. 7: Time-dependent change in the concentration of H_2O_2, NO_2^-, NO_3^-, and O_2 in DI water treated directly with the He APPJ (without agarose) or through an agarose target (with agarose). The He APPJ treatment time was 12 min as highlighted in the graphs.

as shown in Figures 6 and 7, irrespective of the He APPJ treatment time (5 or 12 min). For both He APPJ treatment times, after the lag period, the H_2O_2, NO_3^- and O_2 concentrations increased almost linearly, while the NO_2^- concentration remained relatively constant. The He APPJ delivered relatively lower concentrations of NO_2^- and NO_3^- at 0.05 mg/L or less through agarose into the DI water compared to direct treatment of the water. But a higher concentration of H_2O_2 was delivered into the DI water for the through-agarose treatment at the 30 min time point compared to direct treatment. The O_2 concentration was always equal to or higher than the original O_2 concentration in the DI water with through-agarose treatment (compared to direct treatment). For through-agarose treatment, at the 30 min time point, the O_2 concentration was 10.2 and 12.5 mg/L for 5 and 12 min of He APPJ treatment, respectively.

RONS can enhance or impair cell activity and can induce cytotoxic and genotoxic effects depending on the reactivity, specificity, and dosage of the RONS. For example, micromolar increases in H_2O_2 can stimulate cell proliferation, but higher concentrations of H_2O_2 induce cell death.[14] Reuter et al.[61] demonstrated the differential effects between plasma-generated ROS and RNS on HaCaT cell viability in vitro. Dröge discussed in detail the roles of RONS in physiology and how the dynamic changes in RONS help the body fight against disease, such as during inflammation.[72] Therefore, it will be essential to know the type, concentration, and delivery depth of RONS within tissue fluid and tissue in order to develop safer and more effective plasma devices and protocols, and to improve our understanding of the mechanisms of plasma in medicine.

IV. CONCLUSIONS

These experiments demonstrate the time-dependent change in the concentration of H_2O_2, NO_2^-, NO_3^- and O_2 in DI water treated with a He APPJ directly, or through a 1.5 mm thick agarose target as a surrogate for tissue. The He APPJ generated RONS directly in the DI water through a much faster process compared to treatment through the agarose target. H_2O_2 is the major RONS generated for both direct and through-agarose treatments. For direct treatment, RONS were generated in the DI water only during the He APPJ treatment, whereas for through-agarose treatment, RONS were continually transported into the DI water long after (25 min) the plasma and He gas flow were switched off. The He APPJ deoxygenated the DI water upon direct contact but oxygenated the DI water for treatment through the agarose target. These results have implications for plasma medicine, where for reasons of patient safety, defined doses of plasma will eventually be mandated. Herein, we show that APPJ treatment results in dynamic changes in the RONS concentration and composition and in O_2 concentration within an agarose target. These need to be understood, as they have the potential to significantly affect the medical outcome.

ACKNOWLEDGMENTS

This work was supported by Priority Research Grant of Kochi University of Technology and also by Wound Management Innovation CRC (project RP 2.11).

REFERENCES

1. Becker KH, Kogelschatz U, Schoenbach KH, Barker RJ. Non-equilibrium air plasmas at atmospheric pressure. Philadelphia: IOP Publishing; 2005.
2. Tachibana K. Current status of microplasma research. IEEJ Trans. 2006;1:145–55.
3. Oh J-S, Szili EJ, Gaur N, Hong S-H, Furuta H, Short RD, Hatta A. In-situ UV absorption spectroscopy for monitoring transport of plasma reactive species through agarose as surrogate for tissue. J Photopolym Sci Technol. 2015;28(3):439–44.
4. Szili EJ, Oh J-S, Hong S-H, Hatta A, Short RD. Probing the transport of plasma-generated RONS in an agarose target as surrogate for real tissue: dependency on time, distance and material composition. J Phys D: Appl Phys. 2015;48(20):202001.
5. Iza F, Kim GJ, Lee SM, Lee JK, Walsh JL, Zhang YT, Kong MG. Microplasmas: sources, particle kinetics, and biomedical applications. Plasma Process Polym. 2008;5(4):322–44.
6. Fridman G, Friedman G, Gutsol A, Shekhter AB, Vasilets VN, Fridman A. Applied plasma medicine. Plasma Process Polym. 2008;5(6):503–33.
7. Kong MG, Kroesen G, Morfill G, Nosenko T, Shimizu T, Van Dijk J, Zimmermann JL. Plasma medicine: an introductory review. New J Phys. 2009;11:115012.
8. Laroussi M. Low-temperature plasmas for medicine? IEEE Trans Plasma Sci. 2009;37(6):714–25.
9. Morfill GE, Kong MG, Zimmermann JL. Focus on plasma medicine. New J Phys. 2009;11:115011.
10. Weltmann KD, Kinde E, Von Woedtke T, Hähnel M, Stieber M, Brandenburg R. Atmospheric-pressure plasma sources—prospective tools for plasma medicine. Pure Appl Chem. 2010;82(6):1223–37.
11. Von Woedtke T, Reuter S, Masur K, Weltmann K-D. Plasmas for medicine. Phys Rep. 2013;530(4):291–320.
12. Laroussi M. From killing bacteria to destroying cancer cells: 20 years of plasma medicine. Plasma Process Polym. 2014;11(12):1138–41.
13. Graves DB, Hamaguchi S, O'Connell D. In focus: plasma medicine. Biointerphases. 2015;10(2):029301.
14. Halliwell B, Gutteridge JMC. Free radicals in biology and medicine. 4th ed. New York: Oxford University Press; 2007.
15. Graves DB. The emerging role of reactive oxygen and nitrogen species in redox biology and some implications for plasma applications to medicine and biology. J Phys D: Appl Phys. 2012;45(26):263001.
16. Stoffels E, Aranda-Gonzalvo Y, Whitmore TD, Seymour DL, Rees JA. Mass spectrometric detection of short-living radicals produced by a plasma needle. Plasma Sources Sci Technol. 2007;16(3):549–56.
17. McKay K, Oh J-S, Walsh JL, Bradley JW. Mass spectrometric diagnosis of an atmospheric pressure helium microplasma jet. J Phys D: Appl Phys. 2013;46(46):464018.
18. Oh J-S, Furuta H, Hatta A, Bradley JW. Investigating the effect of additional gases in an atmospheric-pressure helium plasma jet using ambient mass spectrometry. Jpn J Appl Phys. 2015;54(1):01AA03.
19. Teschke M, Kedzierski J, Finantu-Dinu EG, Korzec D, Engemann J. High-speed photographs of a dielectric barrier atmospheric pressure plasma jet. IEEE Trans Plasma Sci. 2005;33(2):310–1.

20. Walsh JL, Kong MG. Room-temperature atmospheric argon plasma jet sustained with submicrosecond high-voltage pulses. Appl Phys Lett. 2007;91(22):221502.
21. Mericam-Bourdet N, Laroussi M, Begum A, Karakas E. Experimental investigations of plasma bullets. J Phys D: Appl Phys. 2009;42(5):055207.
22. Karakas E, Akman MA, Laroussi M. Propagation phases of plasma bullets. IEEE Trans Plasma Sci. 2011;39(11):2308–9.
23. Oh J-S, Olabanji OT, Hale C, Mariani R, Kontis K, Bradley JW. Imaging gas and plasma interactions in the surface-chemical modification of polymers using micro-plasma jets. J Phys D: Appl Phys. 2011;44(15):155206.
24. Oh J-S, Aranda-Gonzalvo Y, Bradley JW. Time-resolved mass spectroscopic studies of an atmospheric-pressure helium microplasma jet. J Phys D: Appl Phys. 2011;44(36):365202.
25. Oh J-S, Walsh JL, Bradley JW. Plasma bullet current measurements in a free-stream helium capillary jet. Plasma Sources Sci Technol. 2012;21(3):034020.
26. Uchida G, Takenaka K, Kawabata K, Setsuhara Y. Influence of He gas flow rate on optical emission characteristics in atmospheric dielectric-barrier-discharge plasma jet. IEEE Trans Plasma Sci. 2015;43(3):737–44.
27. Tanaka H, Mizuno M, Ishikawa K, Nakamura K, Kajiyama H, Kano H, Kikkawa F, Hori M. Plasma-activated medium selectively kills glioblastoma brain tumor cells by down-regulating a survival signaling molecule, AKT kinase. Plasma Med. 2011;1(3):265–77.
28. Tanaka H, Mizuno M, Ishikawa K, Nakamura K, Utsumi F, Kajiyama H, Kano H, Maruyama S, Kikkawa F, Hori M. Cell survival and proliferation signaling pathways are downregulated by plasma-activated medium in glioblastoma brain tumor cells. Plasma Med. 2012;2(4):207–20.
29. Utsumi F, Kajiyama H, Nakamura K, Tanaka H, Mizuno M, Ishikawa K, Kondo H, Kano, H, Hori M, Kikkawa F. Effect of indirect nonequilibrium atmospheric pressure plasma on anti-proliferative activity against chronic chemo-resistant ovarian cancer cells in vitro and in vivo. PLoS ONE. 2013;8(12):e81576.
30. Torii K, Yamada S, Nakamura K, Tanaka H, Kajiyama H, Tanahashi K, Iwata N, Kanda M, Kobayashi D, Tanaka C, Fujii T, Nakayama G, Koike M, Sugimoto H, Nomoto S, Natsume A, Fujiwara M, Mizuno M, Hori M, Saya H, Kodera Y. Effectiveness of plasma treatment on gastric cancer cells. Gastric Cancer. 2014;18(3):635–43.
31. Tanaka H, Mizuno M, Ishikawa K, Takeda K, Nakamura K, Utsumi F, Kajiyama H, Kano H, Okazaki Y, Toyokuni S, Maruyama S, Kikkawa F, Hori M. Plasma medical science for cancer therapy: toward cancer therapy using nonthermal atmospheric pressure plasma. IEEE Trans Plasma Sci. 2014;42(12):3760–4.
32. Utsumi F, Kajiyama H, Nakamura K, Tanaka H, Hori M, Kikkawa F. Selective cytotoxicity of indirect nonequilibrium atmospheric pressure plasma against ovarian clear-cell carcinoma. SpringerPlus. 2014;3(1):398.
33. Hattori N, Yamada S, Tori K, Takeda S, Nakamura K, Tanaka H, Kajiyama H, Kanda M, Fuji T, Nakayama G, Sugimoto H, Koike M, Nomoto S, Fujiwara M, Mizuno M, Hori M, Kodera Y. Effectiveness of plasma treatment on pancreatic cancer cells. Int J Oncol. 2015;47(5):1655–62.
34. Lloyd G, Friedman G, Jafri S, Schultz G, Fridman A, Harding K. Gas plasma: medical uses and developments in wound care. Plasma Process Polym. 2010;7(3-4):194–211.
35. Salehi S, Shokri A, Khani M R, Bigdeli M, Shokri B. Investigating effects of atmospheric-pressure plasma on the process of wound healing. Biointerphases. 2015;10(2):029504.

36. Doherty KG, Oh J-S, Unsworth P, Bowfield A, Sheridan CM, Weightman P, Bradley JW, Williams RL. Polystyrene surface modification for localized cell culture using a capillary dielectric barrier discharge atmospheric-pressure microplasma jet. Plasma Process Polym. 2013;10(11):978–89.
37. Szili EJ, Al-Bataineh SA, Bryant PM, Short RD, Bradley JW, Steele DA. Controlling the spatial distribution of polymer surface treatment using atmospheric-pressure microplasma jets. Plasma Process Polym. 2011;8(1):38–50.
38. Oh J-S, Kakuta Y, Yasuoka Y, Furuta H, Hatta A. Localized DLC etching by a non-thermal atmospheric-pressure helium plasma jet in ambient air. Diamond Relat Mater. 2014;50:91–6.
39. Szili EJ, Bradley JW and Short RD. A 'tissue model' to study the plasma delivery of reactive oxygen species. J Phys D: Appl Phys. 2014;47(15):152002.
40. Laroussi M. From killing bacteria to destroying cancer cells: 20 years of plasma medicine. Plasma Process Polym. 2014;11(12):1138–41.
41. Ratovitski EA, Cheng X, Yan D, Sherman JH, Canady J, Trink B, Keidar M. Anti-cancer therapies of 21st century: novel approach to treat human cancers using cold atmospheric plasma. Plasma Process Polym. 2014;11(12):1128–37.
42. Graves DB. Reactive species from cold atmospheric plasma: implications for cancer therapy. Plasma Process Polym. 2014;11(12):1120–7.
43. Niemira BA, Boyd G, Sites J. Cold plasma rapid decontamination of food contact surfaces contaminated with Salmonella biofilms. J Food Sci. 2014;79(5): M917–M922.
44. Alkawareek MY, Algwari QT, Laverty G, Gorman SP, Graham WG, O'Connell D, Gilmore BF. Eradication of Pseudomonas aeruginosa biofilms by atmospheric pressure non-thermal plasma. PLoS ONE. 2012;7:e44289.
45. Xiong Z, Du T, Lu X, Cao Y, Pan Y. How deep can plasma penetrate into a biofilm? Appl Phys Lett. 2011;98(22):221503.
46. Pei X, Lu X, Liu J, Liu D, Yang Y, Ostrikov K, Chu PK, Pan Y. Inactivation of a 25.5 μm Enterococcus faecalis biofilm by a room-temperature, battery-operated, handheld air plasma jet. J Phys D: Appl Phys. 2012;45(16):165205.
47. Sladek REJ, Filoche SK, Sissons CH, Stoffels E. Treatment of Streptococcus mutans biofilms with a nonthermal atmospheric plasma. Lett Appl Microbiol. 2007;45(3):318–23.
48. Becker K, Koutsospyros A, Yin SM, Christodoulatos C, Abramzon N, Joaquin JC, Brelles-Marino G. Environmental and biological applications of microplasmas. Plasma Phys Contr F. 2005;47(12B):B513.
49. Keidar M, Walk R, Shashurin A, Srinivasan P, Sandler A, Dasgupta S, Ravi R, Guerrero-Preston R, Trink B. Cold plasma selectivity and the possibility of a paradigm shift in cancer therapy. Br J Cancer. 2011;105(9):1295–301.
50. Keidar M, Shashurin A, Volotskova O, Stepp MA, Srinivasan P, Sandler A, Trink B. Cold atmospheric plasma in cancer therapy. Phys Plasmas. 2013;20:057101.
51. Gaur N, Szili EJ, Oh J-S, Hong S-H, Graves DB, Hatta A, Short RD. Combined effect of protein and oxygen on reactive oxygen and nitrogen species in the plasma treatment of tissue. Appl Phys Lett. 2015;107(10):103703.
52. Scionti G, Moral M, Toledano M, Osorio R, Durán JDG, Alaminos M, Campos A, López-López MT. Effect of the hydration on the biomechanical properties in a fibrin-agarose tissue-like model. J Biomed Mater Res A. 2014;102(8):2573–82.
53. Pomfret R, Sillay K, Miranpuri G. Investigation of the electrical properties of agarose gel: characterization of concentration using Nyquist plot phase angle and the implications of a

more comprehensive in vitro model of the brain. Ann Neurosci. 2013;20(3):99–107.
54. Chen Z-J, Gillies GT, Broaddus WC, Prabhu SS, Fillmore H, Mitchell RM, Corwin FD, Fatouros PP. A realistic brain tissue phantom for intraparenchymal infusion studies. J Neurosurg. 2004;101(2):314–22.
55. Kato H, Ishida T. Development of an agar phantom adaptable for simulation of various tissues in the range 5-40 MHz. (Hyperthermia treatment of cancer). Phys Med Biol. 1987;32(2):221–6.
56. Hildebrand P, Kleemann M, Roblick U, Mirow L, Bruch H-P, Bürk C. Development of a perfused ex vivo tumor-mimic model for the training of laparoscopic radiofrequency ablation. Surg Endosc. 2007;21(10):1745–9.
57. Scott D, Young W, Watumull L, Lindberg G, Fleming J, Rege R, Brawn R, Jones D. Development of an in vivo tumor-mimic model for learning radiofrequency ablation. J Gastrointest Surg. 2000;4(6):620–5.
58. Taylor GD, Cadeddu JA. Training for renal ablative technique using an agarose-based renal tumour-mimic model. BJU Int. 2006;97(1):179–81.
59. Dobrynin D, Fridman G, Friedman G, Fridman A. Deep penetration into tissues of reactive oxygen species generated in floating-electrode dielectric barrier discharge (FE-DBD): an in vitro agarose gel model mimicking an open wound. Plasma Med. 2012;2(1-3):71–83.
60. Park D, Fridman G, Fridman A, Dobrynin D. Plasma bullets propagation inside of agarose tissue model. IEEE Trans Plasma Sci. 2013;41:1725–30.
61. Reuter S, Tresp H, Wende K, Hammer MU, Winter J, Masur K, Schmidt-Bleker A, Weltmann K. From RONS to ROS: tailoring plasma jet treatment of skin cells. IEEE Trans Plasma Sci. 2012; 40(9): 2986–93.
62. Naïtali M, Kamgang-Youbi G, Herry J-M, Bellon-Fontaine M-N, Brisset J-L. Combined effects of long-living chemical species during microbial inactivation using atmospheric plasma-treated water. Appl Environ Microbiol. 2010;76(22):7662–4.
63. Ercan UK, Wang H, Ji H, Fridman G, Brooks AD, Joshi SG. Nonequilibrium plasma-activated antimicrobial solutions are broad-spectrum and retain their efficacies for extended period of time. Plasma Process Polym. 2013;10(7): 544–55.
64. Julák J, Scholtz V, Kotúčová S, Janoušková O. The persistent microbicidal effect in water exposed to the corona discharge. Phys Med. 2012;28(3):230–9.
65. Oehmigen K, Hähnel M, Brandenburg R, Wilke C, Weltmann KD, von Woedtke T. The role of acidification for antimicrobial activity of atmospheric pressure plasma in liquids. Plasma Process Polym. 2010;7(3-4):250–7.
66. Traylor MJ, Pavlovich MJ, Karim S, Hait P, Sakiyama Y, Clark DS, Graves DB. Long-term antibacterial efficacy of air plasma-activated water. J Phys D: Appl Phys. 2011;44(47):472001.
67. Collet G, Robert E, Lenoir A, Vandamme M, Darny T, Dozias S, Kieda C, Pouvesle JM. Plasma jet-induced tissue oxygenation: potentialities for new therapeutic strategies. Plasma Sources Sci Technol. 2014;23(1):012005.
68. Hatta A, Oh J-S. Curve-fitting program (unpublished).
69. Tian W, Kushner MJ. Atmospheric pressure dielectric barrier discharges interacting with liquid covered tissue. J Phys D: Appl Phys. 2014;47(16):165201.
70. Attri P, Kim Y-H, Park D-H, Park J-H, Hong Y-J, Uhm H-S, Kim K-N, Fridman A, Choi E-H. Generation mechanism of hydroxyl radical species and its lifetime prediction during the plasma-initiated ultraviolet (UV) photolysis. Sci Rep. 2015;5:9332.
71. Oh J-S, Ito S, Furuta H, Hatta A. Time-resolved in situ UV absorption spectroscopic stud-

ies for detection of reactive oxygen and nitrogen species (RONS) in plasma activated water, 22nd International Symposium on Plasma Chemistry (ISPC-22); July 5–10, 2015; Antwerp, Belgium.
72. Dröge W. Free radicals in the physiological control of cell function, Physiol. Rev. 2002;82:47–95.